IAEA
International Atomic Energy Agency

20th IAEA Fusion Energy Conference
Vilamoura, Portugal, 1-6 November 2004

IAEA-CN-116/TH/P4-46

External mode analysis in a tokamak by the Newcomb Equation

S. Tokuda[1], N. Aiba[2], and M. Okamoto[3]
[1] Naka Fusion Research Establishment, JAERI, Naka, Ibaraki 311-0193, Japan
[2] The Graduate University for Advanced Studies, Toki, Gifu 509-5292, Japan
[3] National Institute for Fusion Science, Toki, Gifu 509-5292, Japan
e-mail contact of main author: tokudas@koma.jaeri.go.jp

External mode analysis in a tokamak by the Newcomb equation

S. Tokuda[1], N. Aiba[2], and M. Okamoto[3]

[1] Naka Fusion Research Establishment, JAERI, Naka, Ibaraki 311-0193, Japan
[2] The Graduate University for Advanced Studies, Toki, Gifu 509-5292, Japan
[3] National Institute for Fusion Science, Toki, Gifu 509-5292, Japan

E-mail: tokudas@koma.jaeri.go.jp

Abstract. Recent progress in the theory of the Newcomb equation is reported. Emphasis is put on the analysis of external modes including peeling modes (high n kink modes), where n is the toroidal mode number. A theory for low n external modes is developed so that it is also useful for the analysis of resistive wall modes.

1. Introduction

It is well known that the Newcomb equation, the inertia free linear ideal magnetohydrodynamic (MHD) equation[1], plays fundamental roles in the MHD stability theory. A code MARG2D has been developed which solves numerically the 2-dimensional (2-D) Newcomb equation and the associated eigenvalue problem[2]. In this paper, recent research on the 2-D Newcomb equation is reported. The main focus is to develop tools for the analysis of low n and high n external modes, where n is the toroidal mode number. The high n kink modes, called peeling modes[3], recently get attention in the study on MHD stability of tokamak edge plasmas[4]. For the low n external modes, we develop a theory that expresses the change of potential energy due to the plasma displacement by a quadratic form with respect to the values of the displacement at the plasma surface. This formulation is useful for the analysis of resistive wall modes. For the analysis of peeling modes we extend the MARG2D formulation into the vacuum region by expressing the perturbation of magnetic fields in vacuum by a suitable vector potential.

2. Newcomb equation

In an axisymmetric toroidal system such as a tokamak, equilibrium magnetic fields are expressed as

$$\mathbf{B}_{\rm eq} = \nabla\phi \times \nabla\psi + F\nabla\phi, \tag{1}$$

where the cylindrical coordinate system (R, Z, ϕ) is employed; $\psi(R, Z)$ and $F(\psi)$ are, respectively, the poloidal flux function and toroidal field function. We define the radial coordinate by

$$r^2 := 2R_0 \int_0^{\psi} \frac{q}{F} d\psi. \tag{2}$$

Here, R_0 is the position of the magnetic axis (for simplicity, the mirror symmetry of the equilibrium is assumed: $\psi(R, -Z) = \psi(R, Z)$); $q(r)$ is the safety factor, as usual. We define the poloidal angle θ so that the magnetic field lines are straight; the Jacobian of the coordinate system (r, θ, ϕ) is $\sqrt{g} = rR^2/R_0$. Let $\vec{\zeta}$ be an infinitesimal plasma displacement with the toroidal mode number n that is incompressible ($\nabla \cdot \vec{\zeta} = 0$), and let

$$X(r,\theta) := \vec{\zeta} \cdot \nabla r, \quad V(r,\theta) := r(\vec{\zeta} \cdot \nabla\theta - \frac{1}{q}\vec{\zeta} \cdot \nabla\phi), \tag{3}$$

then the change of the plasma potential energy W_p due to the displacement $\vec{\zeta}$ reads[5]

$$W_p = \pi \int \mathcal{L} dr d\theta, \tag{4}$$

and the Lagrangian density function $\mathcal{L}$ reads

$$\begin{aligned} \mathcal{L} &= a|D_\theta(X)|^2 + c|\partial_r(rX) + \partial_\theta V|^2 + e|X|^2 \\ &+ b|inV + \frac{1}{q}\partial_r(rX) + hX + r\beta_{r\theta} D_\theta(X)|^2. \end{aligned} \tag{5}$$

Here, the operator $D_\theta(X)$ is defined by

$$D_\theta(X) := \frac{1}{q}\partial_\theta X - inX, \tag{6}$$

and the other coefficients are given in Ref.[2].
By minimizing W_p with respect to $V(r,\theta)$, we obtain the reduced energy integral

$$W_p[\mathbf{X},\mathbf{X}] = 2\pi^2 \int_0^a L[\mathbf{X},\mathbf{X}] dr. \tag{7}$$

Here, the vector function $\mathbf{X}(r)$ is defined as

$$\mathbf{X}(r) := \{X_{-L_f}(r), \cdots, X_{L_f}(r)\}^t, \tag{8}$$

by using the poloidal Fourier harmonics $X_l(r)$

$$X(r,\theta) = \sum_{l=-L_f}^{L_f} X_l(r) \exp(il\theta), \tag{9}$$

where L_f is the truncated poloidal mode number. And the reduced Lagrangian density is

$$L[\mathbf{X},\mathbf{X}] = \langle \frac{d\mathbf{X}}{dr}|\boldsymbol{L}|\frac{d\mathbf{X}}{dr}\rangle + \langle \mathbf{X}|\boldsymbol{K}|\mathbf{X}\rangle + \langle \frac{d\mathbf{X}}{dr}|\boldsymbol{M}^t|\mathbf{X}\rangle + \langle \mathbf{X}|\boldsymbol{M}|\frac{d\mathbf{X}}{dr}\rangle, \tag{10}$$

where $\boldsymbol{L}, \boldsymbol{M}, \boldsymbol{K}$ are matrices; $\boldsymbol{L}$ and $\boldsymbol{K}$ are hermitian, the details of which are given in Ref[2], and

$$\langle \mathbf{X}|\boldsymbol{K}|\mathbf{X}\rangle := \sum_{j,k} X_j K_{jk} X_k.$$

From $L[\mathbf{X},\mathbf{X}]$, we have the 2-D Newcomb equation

$$\mathcal{N}\mathbf{X} := -\frac{d}{dr}\left(\boldsymbol{L}\frac{d\mathbf{X}}{dr}\right) - \frac{d}{dr}(\boldsymbol{M}^t\mathbf{X}) + \boldsymbol{M}\frac{d\mathbf{X}}{dr} + \boldsymbol{K}\mathbf{X} = 0. \tag{11}$$

The eigenvalue problem associated with Eq.(11) is given by

$$\mathcal{N}\mathbf{X} = -\lambda\mathcal{R}\mathbf{X}, \tag{12}$$

where $\mathcal{R}$ is a multiplicative and diagonal operator whose components are $R_{m,m} \propto (m/q - n)^2$. The natural boundary condition for X_m is imposed at the rational surface of r_m ($m = nq(r_m)$); the continuous conditions are imposed for other harmonics X_l ($l \neq m$). A code MARG2D which solves Eqs.(11, 12) has been developed by using a finite element method. The code has been applied to identify stable states for ideal MHD internal perturbations[2].

3. Application to the theory of low n external modes

The bilinear form associated with Eq.(7) is given by

$$W[\vec{\xi},\vec{\eta}] = W_p[\vec{\xi},\vec{\eta}] + \langle \vec{\xi}_a|\boldsymbol{M}_V|\vec{\eta}_a\rangle, \tag{13}$$

where $\vec{\xi}_a = \vec{\xi}(a)$ and the matrix $\boldsymbol{M}_V$ stands for the contribution from the vacuum region. Let $S = \{\vec{\xi} \mid \mathcal{N}\vec{\xi} = 0\}$ be a set of functions that satisfy the Newcomb equation. If $\vec{\xi}(r), \vec{\eta}(r) \in S$, then we have

$$W_p[\vec{\xi},\vec{\eta}] = \langle \vec{\xi}_a|\boldsymbol{M}_H|\vec{\eta}_a\rangle + \frac{1}{2}\left\langle \vec{\xi}_a|\boldsymbol{L}|\frac{d\vec{\eta}_a}{dr}\right\rangle + \frac{1}{2}\left\langle \frac{d\vec{\xi}_a}{dr}|\boldsymbol{L}|\vec{\eta}_a\right\rangle, \tag{14}$$

$$\boldsymbol{M}_H := \frac{1}{2}(\boldsymbol{M} + \boldsymbol{M}^t). \tag{15}$$

Now let us make a vector function $\vec{Y}^m(r) \in S$

$$\vec{Y}^m(r) = (Y^m_{-L_f}(r), \cdots, Y^m_{L_f}(r))^t, \tag{16}$$

for $m = 0, \pm 1, \cdots, \pm L_f$, where each poloidal harmonics $Y^m_l(r)$ satisfies the condition

$$Y^m_l(a) = 0 \quad (l \neq m), \quad Y^m_m(a) = 1, \;\; l = 0, \pm 1, \cdots, \pm L_f. \tag{17}$$

The set $\{\vec{Y}^m(r)\}$ forms a basis[6]. An external mode can be expressed by using an arbitrary set $\{x_m\}$ of real numbers as

$$\vec{\xi}(r) = \sum_m x_m \vec{Y}^m(r). \tag{18}$$

The change of the potential energy due to $\vec{\xi}$ is given by the vector $\vec{x}$ as

$$W[\vec{\xi},\vec{\xi}] = \langle \vec{x}|\boldsymbol{A}|\vec{x}\rangle, \tag{19}$$

where the matrix $\boldsymbol{A}$, which is real and symmetric, is given by

$$\boldsymbol{A} = \boldsymbol{M}_p + \boldsymbol{M}_V, \;\; M_{p(l,m)} = W_p[\vec{Y}^l, \vec{Y}^m]. \tag{20}$$

We call $\boldsymbol{A}$ the stability matrix for external modes. If the minimum eigenvalue of $\boldsymbol{A}$ is negative, then the plasma is unstable against ideal external kink modes. The matrix $\boldsymbol{A}$ also plays an important role in the stability of resistive wall modes[6].

The basis $\{\vec{Y}^m(r)\}$ can be constructed by using the response formalism[7]. Let us write $\vec{Y}^m(r)$ as

$$\vec{Y}^m(r) = \vec{X}^m(r) + \vec{Z}^m(r), \tag{21}$$

where $\vec{Z}^m(r)$ given analytically satisfies the inhomogenous boundary condition, Eq.(17). Then, we have an inhomogeneous equation for $\vec{X}^m(r)$ with the homogenous boundary condition

$$\mathcal{N}\vec{X}^m(r) = -\mathcal{N}\vec{Z}^m(r), \quad \vec{X}^m(a) = 0. \tag{22}$$

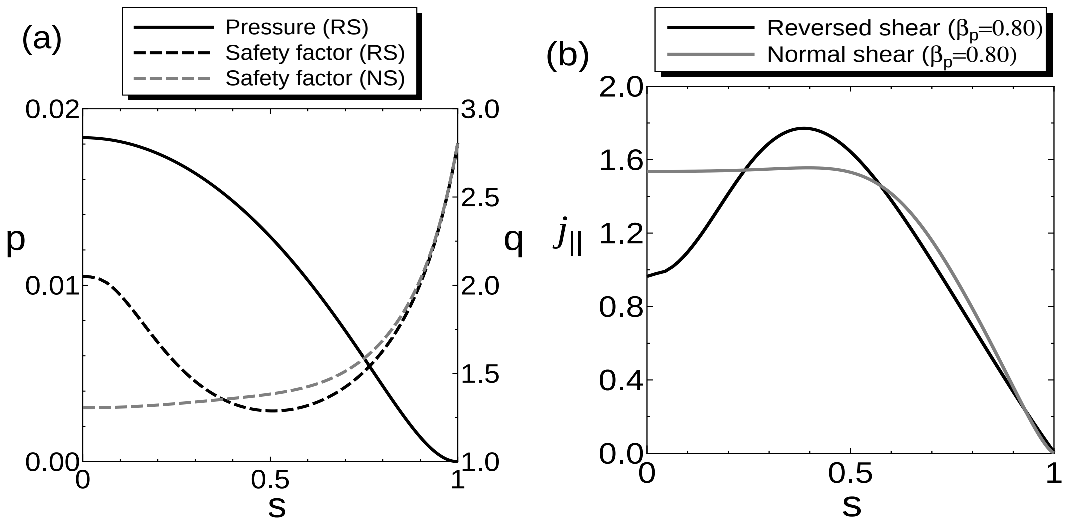

FIG. 1. (a) Profiles of the pressure p and the safety factor q of RS and the q profile of NS. The β_p of these equilibria are 0.80. The values of q_{min} and q_a in RS are same as those in NS ($q_{min} = 1.30$, $q_a = 2.80$). (b) Profile of the parallel current density $j_\parallel$ of RS and that of NS. These profile near the plasma surface are similar to each other.

Since Eq.(22) can be solved by the MARG2D code, we can construct the basis $\{\vec{Y}^m(r)\}$ and the stability matrix $\boldsymbol{A}$.

The present formalism enables us to get deeper insight into the stability properties of external modes when it is combined with the eigenvalue problem associated with the original Newcomb equation[8]. It clarifies that the stable internal modes can destabilize the external modes and change the surface mode structure of external modes into a global mode structure. The difference in the stability properties between the normal shear tokamak (NS) and a reversed shear tokamak (RS), as shown in Fig.1, can be analyzed from such a viewpoint. Fig.2 shows the q_a dependence of μ_0, the minimun eigenvalue of the matrix $\boldsymbol{A}$, and λ_{0-int}, the minimum eigenvalue of the eigenvalue problem associated with the Newcomb equation with the fixed boundary condition. The black solid line and the black dashed line show μ_0 and λ_{0-int} in RS, and the gray solid line and the gray dashed line are for μ_0 and λ_{0-int} in NS. In the region $4.50 < q_a$, μ_0's for RS and NS are nearly identical. When q_a has a high value, low-n external modes are surface modes, and the stability is mostly determined by the magnetic shear and $j_\parallel$ profiles near the plasma surface, and internal modes have little effects on the stability of external modes.

We see the high-β_p RS equilibria still have a stable window against external modes, $3.00 < q_a < 3.52$, although the high-β_p NS equilibria are unstable when $q_a < 4.28$. Since the destabilizing effects of the current density near the plasma surface in both equilibria are considered as almost same, such stabilization should reflect the difference of the stability of internal modes, which is caused by the different q profiles. Figure 3 shows the poloidal Fourier harmonics of the eigenfunction belonging to μ_0 (fig.3(a)) and those of the eigenfunction belonging to λ_{0-int} (fig.3(b)) when $q_a = 3.53$ in RS; this q_a is close to $q_{a-mgl} = 3.52$ that is the marginally stable q_a for external modes in RS. These figures imply that the internal mode whose harmonics are $l \leq 3$ destabilize the external mode with the $l \geq 4$ harmonics peaking at the plasma surface. However, internal modes in RS are more stable than those in NS when $3.00 < q_a < 4.50$, and as the result, the effect of internal modes on the stability of external modes in RS is weaker than that in NS.

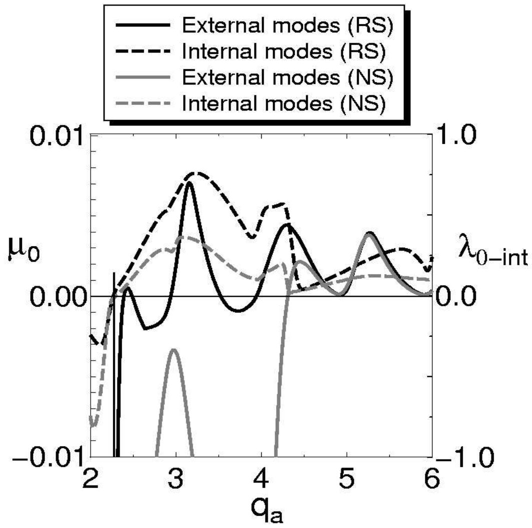

FIG. 2. Dependence of μ_0 on q_a and that of λ_{0-int} on q_a in RS, and those in NS. The spectral structure for external modes in RS when $q_a \geq 4.50$ is almost indistinguishable with that in NS. It is because the destabilizing effects for $q_a \geq 4.50$ are almost same as each other. In RS, a stable window against external modes exists in lower q_a, $3.00 \leq q_a \leq 3.53$.

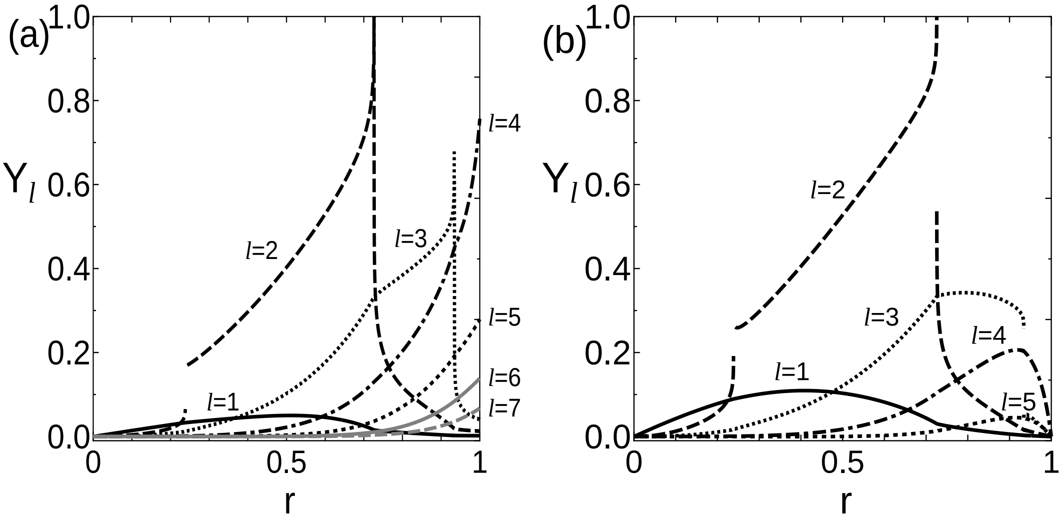

FIG. 3. (a) Poloidal Fourier harmonics of the eigenfunction belonging to the minimum eigenvalue of the stability matrix (external modes), and (b) those of the eigenfunction belonging to the minimum eigenvalue obtained by solving 12 with the fixed boundary condition (internal modes), in the $\beta_p = 0.80$ and $q_a = 3.53$ RS. The profile of $l \leq 3$ harmonics in figure (a) are similar to that in figure (b), and these harmonics destabilize external modes.

4. Extension of the MARG2D formulation into the vacuum

The vacuum contribution to the change of potential energy is represented by the matrix $\boldsymbol{M}_V$ in Eq.(13), which is computed by using Green's function of the Laplace operator[9]. This method deals flexibly with the shape of a conducting wall. However, the method is limited to low n modes since it is difficult to evaluate numerically special functions that appear in constructing $\boldsymbol{M}_V$ when n becomes large. It is convenient to express magnetic fields by a vector potential for middle n ($n = 2, 3, \cdots, 10$) or high n ($n > 10$) external modes, which was shown in Ref.[10]. We adopt the vector potential method in the MARG2D code for the analysis of peeling modes. It is shown that the Lagrangian density function for the change of energy in the vacuum has the same form as that for the change of plasma potential energy, and that the MARG2D formulation is easily extended to such external modes.
Let $\psi_V(R, Z)$ be a function defined in the vacuum. The coutour $\psi_V(R, Z) = \psi_s$ coincides with the plasma surface $\psi(R, Z) = \psi_s$. We also assume that the outermost contour of $\psi_V(R, Z) = const.$ coincides with the cross section of the conducting wall. Next, we introduce a vector field $\mathbf{C}_V$ in the vacuume by

$$\mathbf{C}_V = \nabla\phi \times \nabla\psi_V + T_V(R, Z)\nabla\phi. \tag{23}$$

Here we assume T_V is independent of ϕ. It is easy to see that $\mathbf{C}_V$ is a solenoidal vector[10], $\mathrm{div}\mathbf{C}_V = 0$. The poloidal angle θ and the function T_V can be defined such that

$$\frac{\mathbf{C}_V \cdot \nabla\phi}{\mathbf{C}_V \cdot \nabla\theta} = q_s(= const.), \tag{24}$$

at all points in the vacuum, where q_s is the safety factor at the edge.
The perturbation of magnetic fields is given by

$$\mathbf{B} = \nabla \times \mathbf{A}, \quad \mathbf{A} = \vec{\xi}_V \times \mathbf{C}_V, \tag{25}$$

where $\vec{\xi}_V$ is the unknown vector to be determined. By introducing the functions

$$Y(\psi_V, \theta) := \vec{\xi}_V \cdot \nabla\psi_V, \quad V(\psi_V, \theta) := \vec{\xi}_V \cdot \nabla\theta - \frac{1}{q_s}\vec{\xi}_V \cdot \nabla\phi, \tag{26}$$

the change of energy in the vacuum is given by

$$W_V = \pi q_s \int \mathcal{L} d\psi_V d\theta, \tag{27}$$

$$\mathcal{L} = a_V|D_\theta(Y)|^2 + c_V|\frac{\partial V}{\partial\theta} + \frac{\partial Y}{\partial\psi_V}|^2 + b_V|inq_sV + \frac{\partial Y}{\partial\psi_V}\beta_{\psi\theta}D_\theta(Y)|^2. \tag{28}$$

Here

$$D_\theta(Y) := (\frac{1}{q_s}\partial_\theta - in)Y, \quad \beta_{\psi\theta} := \frac{\nabla\psi_V \cdot \nabla\theta}{|\nabla\psi_V|^2}, \tag{29}$$

and

$$a_V := \frac{q_s^2}{|\nabla\psi_V|^2}\frac{1}{\sqrt{g_V}}, \quad b_V := q_s^2\frac{|\nabla\psi_V|^2}{R^2}\sqrt{g_V}, \quad c_V := q_s^2\frac{R^2}{\sqrt{g_V}}. \tag{30}$$

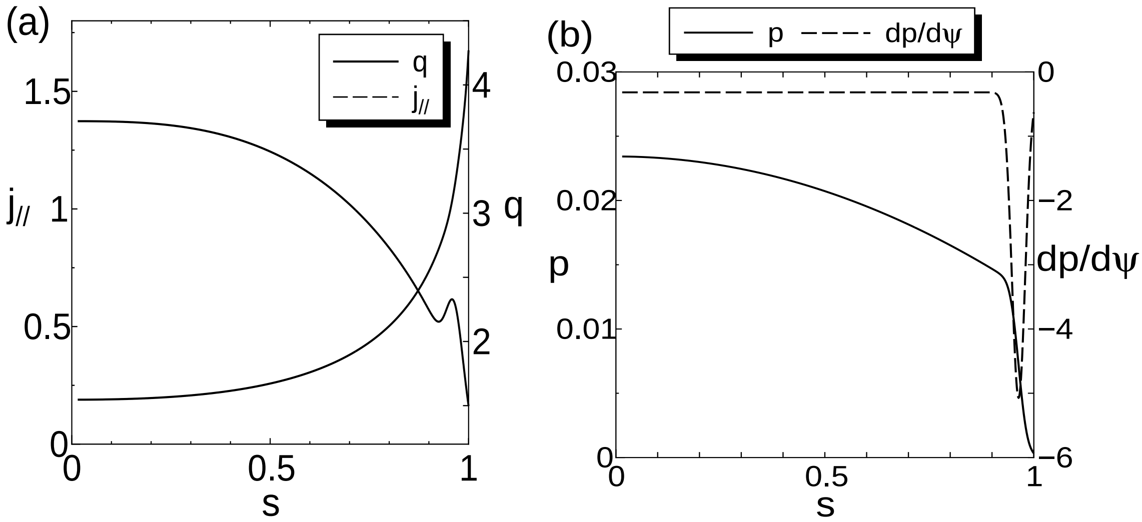

FIG. 4. Equilibrium whose parameters are $A = 3.3$, $\kappa = 1.8$, $\delta = 0.45$, and $\beta_p = 1.2$. (a) Profiles of q (solid line) and $j_{\parallel}$ (dashed line). The values of q_0 and q_a are 1.7 and 4.27, and $j_{\parallel}|_a/\langle j\rangle_a = 0.135$, respectively. (c) Profiles of p (solid line) and $dp/d\psi$ (dashed line).

We can eliminate the function V by the same procedure in Sec.2 by using the poloidal Fourier harmonics

$$Y(\psi_V, \theta) = \sum_l Y_l(\psi_V) \exp(il\theta). \tag{31}$$

Bechmark tests between the MARG2D code and the ERATO code have been excuted for low n ($n = 1 \sim 5$) external kink modes. They showed that both codes correctly capture the external modes, and however, it becomes hard for the ERATO code to identify the β limit against higher n modes since $\lambda(\beta)$ computed from the ERATO code is tangent to the $\beta-$axis ($\lambda = 0$ line). Such behavior of the ERATO code has been well known. On the other hand, $\lambda(\beta)$ computed from the MARG2D code is analytic near the marginal stability, $\lambda(\beta) \propto \beta - \beta_{cr}$, and then it is easy to identify the β limit numerically.
The MARG2D code can capture high n edge modes for an equilibrium with a steep pressure gradient and a finite value of $j_{\parallel}|_a$ near the plasma surface as shown in Fig.4; $A = 3.3, \kappa = 1.8, \delta = 0.45$ and $q_0 = 1.7, q_a = 4.27$. Figure 5 shows the poloidal Fourier harmonics of the unstable eigenfunction of the $n = 40$ mode for $\beta_{\rm p} = 1.4$. The harmonics are packed near the plasma surface with a peeling component of $m = 171$ because $nq_a = 170.8$. Such harmonics are shown in Fig.5(b) as functions of $x = nq(s)$. We see the envelope of an edge ballooning mode whose maxima is $nq \simeq 150$.

5. Summary

We have reported a unified approach to the stability analysis of external MHD modes based on the theory of the Newcomb equation. Such an approach is useful for the analysis of resistive wall modes, and also enables us to analyze the stability of the edge MHD modes with low n to high n modes by using the same code MARG2D.

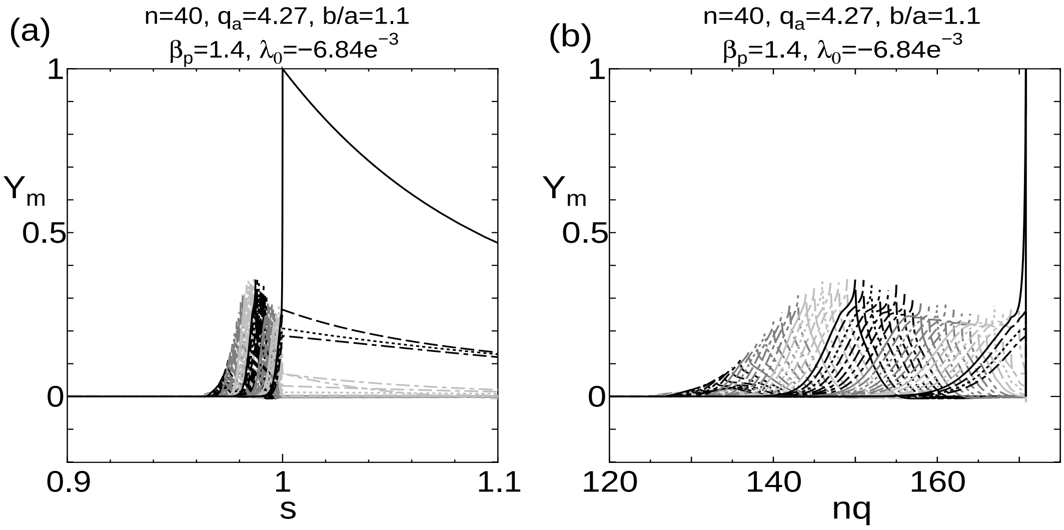

FIG. 5. Poloidal Fourier harmonics of the unstable eigenfunction of the $n = 40$ *mode;* $q_a = 4.27, \beta_p = 1.4$*, and* $b/a = 1.1$.

Acknowledgments

The author wish to thank to Dr. H. Ninomiya and Dr. Y. Kishimoto at JAERI for supporting our research.

References:

[1] W. A. Newcomb, Ann. Phys. **10**, 232 (1960).
[2] S. Tokuda and T. Watanabe, Phys. Plasmas **6**, 3012 (1999).
[3] D. Lortz, Nucl. Fusion **15**, 49 (1975).
[4] W. Connor, R. J. Hastie, and H. R. Wilson, Phys. Plasmas **5**, 2687 (1998).
[5] I. B. Bernstein, E. A. Frieman, M. D. Kruskal, and R. M. Kulsrud, Proc. Roy. Soc. (London). **A244**, 17 (1958).
[6] A. H. Boozer, Phys. Plasmas **5**, 3350 (1998).
[7] S. Tokuda and T. Watanabe, J. Plasma Fusion Res. **73**, 1141 (1997).
[8] N. Aiba, S. Tokuda, T. Ishizawa, and M. Okamoto, Plasma Phys. Control. Fusion **46**, 1699 (2004).
[9] R. Gruber , et al., Comput. Phys. Commun. **21**, 323 (1981).
[10] R. Gruber, et al., Comput. Phys. Commun. **24**, 363 (1981).